Rituparna S. Roy[1]
Hosahudya N. Gopi[1]
S. Raghothama[2]
Richard D. Gilardi[3]
Isabella L Karle[3]
Padmanabhan Balaram[1]

[1] *Molecular Biophysics Unit, Indian Institute of Science, Bangalore-560012, India*

[2] *Sophisticated Instruments Facility, Indian Institute of Science, Bangalore-560012, India*

[3] *Laboratory for the Structure of Matter, Naval Research Laboratory, Washington, DC 20375-5341*

Peptide Hairpins with Strand Segments Containing α- and β-Amino Acid Residues: Cross-Strand Aromatic Interactions of Facing Phe Residues

Received 22 December 2004; revised 1 May 2005; accepted 2 May 2005
Published online 13 May 2005 in Wiley InterScience (www.interscience.wiley.com). DOI 10.1002/bip.20294

Abstract: *The incporation of β-amino acid residues into the strand segments of designed β-hairpin leads to the formation of* polar sheets*, since in the case of β-peptide strands, all adjacent carbonyl groups point in one direction and the amide groups orient in the opposite direction. The conformational analysis of two designed peptide hairpins composed of α/β-hybrid segments are described: Boc–Leu–βPhe–Val–D-Pro–Gly–Leu–βPhe–Val–OMe (**1**) and Boc–βLeu–Phe–βVal–D-Pro–Gly–βLeu–Phe–βVal–OMe (**2**). A 500-MHz ^{1}H-NMR (nuclear magnetic resonance) analysis in methanol supports a significant population of hairpin conformations in both peptides. Diagnostic nuclear Overhauser effects (NOEs) are observed in both cases. X-ray diffraction studies on single crystals of peptide **1** reveal a β-hairpin conformation in both the molecules, which constitute the crystallographic asymmetric unit. Three cross-strand hydrogen bonds and a nucleating type II′ β-turn at the D-Pro–Gly segment are observed in the two independent molecules. In peptide **1**, the βPhe residues at positions 2 and 7 occur at the* nonhydrogen-bonding *position, with the benzyl side chains pointing on opposite faces of the β-sheet. The observed aromatic centroid-to-centroid distances are 8.92 Å (molecule A) and 8.94 Å (molecule B). In peptide **2**, the aromatic rings must occupy facing positions in antiparallel strands, in the NMR-derived structure.*

*Peptide **1** yields a normal ''hairpin-like'' CD spectrum in methanol with a minimum at 224 nm. The CD spectrum of peptide **2** reveals a negative band at 234 nm and a positive band at 221 nm,*

Correspondence to: Padmanabhan Balaram; e-mail: pb@mbu.iisc.ernet.in

Contract grant sponsor: Department of Biotechnology, Government of India, National Institutes of Health (NIH), and the office of Naval Research
Contract grant number: GM30902 (NIH)

Biopolymers (Peptide Science), Vol. 80, 787–799 (2005)

suggestive of an exciton split doublet. Modeling of the facing Phe side chains at the hydrogen-bonding position of a canonical β-hairpin suggests that interring separation is ~4.78 Å for the gauche$^+$gauche$^-$ (g^+g^-) rotamer. A previously reported peptide β-hairpin composed of only α-amino acids, Boc–Leu–Phe–Val–D-Pro–Gly–Leu–Phe–Val–OMe also exhibited an anomalous far-UV (ultraviolet) CD (circular dichroism) spectrum, which was interpreted in terms of interactions between facing aromatic chromophores, Phe 2 and Phe 7 (C. Zhao, P. L. Polavarapu, C. Das, and P. Balaram, Journal of the American Chemical Society, 2000, Vol 122, pp. 8228–8231). © 2005 Wiley Periodicals, Inc.† Biopoly 80: 787–799, 2005

This article was originally published online as an accepted preprint. The Published Online date corresponds to the preprint version. You can request a copy of the preprint by emailing the Biopolymers editorial office at biopolymers@wiley.com

Keywords: *peptide hairpins; hybrid peptides; β-peptides; anomalous circular dichroism; cross-strand aromatic interactions; exciton split doublet; peptide crystal structure*

INTRODUCTION

The ability of a centrally positioned D-Pro–Xxx segment to stabilize β-hairpin conformations in short synthetic peptides is well established by NMR studies in solution[1–8] and X-ray diffraction studies in crystals.[9–14] Robust synthetic hairpin scaffolds provide an opportunity to examine the effect of turn stereochemistry on the orientation of the antiparallel strands[14] and to probe cross-strand interactions between side chains placed at facing positions.[14,15] Hybrid peptides incorporating β-, γ-, and δ-amino acid residues in the strand facilitate changes of the local polarity of the sheets.[16–18] In the case of D-Pro–Gly segments, the nucleating turn can adopt either type I′ ($\phi_{i+1} = 60°$, $\psi_{i+1} = 30°$; $\phi_{i+2} = 90°$, $\psi_{i+2} = 0°$) or type II′ ($\phi_{i+1} = 60°$, $\psi_{i+1} = -120°$; $\phi_{i+2} = -80°$, $\psi_{i+2} = 0°$) conformations, since the achiral Gly residue can readily be accommodated at the $i + 2$ positions of both turn types. Sequence variations in the strand segment permit analysis of cross-strand interactions and intrastrand interactions between proximal side chains. The nature of side-chain interactions in ideal β-hairpins is schematically illustrated in Figure 1. In an earlier study, we have characterized a β-hairpin conformation for the peptide Boc–Leu–Phe–Val-D-Pro–Gly–Leu–Phe–Val–OMe, in solution by nuclear magnetic resonance (NMR) spectroscopy.[15] Interestingly, an anomalous circular dichroism (CD) spectrum for this octapeptide was observed in the region 210–240 nm, suggesting cross-strand aromatic interactions.[15] This segment has also been shown to exist as a β-hairpin, when incorporated into a larger 17-residue sequence that adopts a mixed helix–hairpin structure.[10] Similar side-chain interactions were also established in the peptide, Boc–Leu–Phe–Val–Aib–D-Ala—Leu–Phe–Val–OMe, in which an Aib–D-Ala (type I′ β-turn) nucleated a β-hairpin conformation in crystals.[14] To investigate the effects of cross-strand aromatic interactions in β-hairpins, we have designed and

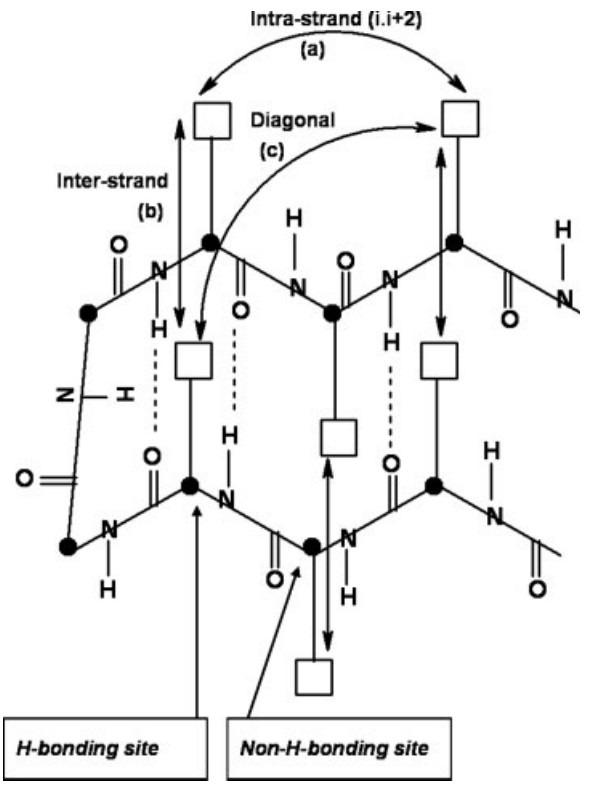

FIGURE 1 Schematic of a peptide β-hairpin indicating the nature of side-chain interactions. (a) The $i/i + 2$ intra-strand interactions and (b) cross-strand interaction between facing residues. Two distinct sites are defined—hydrogen-bonding and nonhydrogen-bonding sites. (c) Cross-strand diagonal interactions.

subjected to conformational analysis the following octapeptides:

1 (Boc–Leu–βPhe–Val– D-Pro–Gly–Leu–βPhe–Val–OMe) [βPhe = (S)-β^3-homophenylalanine].
2 (Boc–βLeu–Phe-βVal–D-Pro–Gly–βLeu–Phe–βVal–OMe) [βLeu = (S)-β^3-homoleucine] and [βVal = (R)-β^3-homovaline].

These sequences were based on the parent peptide Boc–Leu–Phe–Val–D-Pro–Gly–Leu–Phe–Val–OMe (peptide **3**). Replacement of Phe 2 and Phe 7 by βPhe and retention of the β-hairpin conformation should place the two Phe rings on opposite faces of an approximately planar β-sheet structure, eliminating cross-strand interactions. In peptide **2**, replacement of Val 3 and Leu 6 by their higher homologs places the phenyl rings, Phe 2 and Phe 7, at facing *hydrogen-bonded* positions in a β-sheet, in contrast to the parent peptide **3** , where the Phe rings are at facing *no-hydrogen bonded* positions. Peptide **2** also contains β-residues at positions 1 and 8, βLeu and βVal, respectively. This substitution does not affect the aromatic side-chain position but merely alters the sheet polarity at the two termini. The results described in this article establish β-hairpin conformations in solution for both peptides **1** and **2**. In addition, X-ray diffraction studies establish a β-hairpin structure for peptide **1** in crystals. Peptide **1** yields a CD spectrum similar to that normally observed in peptide β-hairpins, while peptide **2** yields an anomalous CD spectrum.

MATERIALS AND METHODS

Peptide Synthesis and Crystallization

The two octapeptides peptide **1** and peptide **2** were synthesized by conventional solution-phase procedures, using a fragment condensation strategy. *t*-Butyloxycarbonyl (Boc) and methyl groups were used for N- and C-terminal protection. Boc–(S)–βPhe–OH, Boc–(S)–βLeu–OH, and Boc–(R)–βVal–OH were synthesized by Arndt–Eistert homologation of Boc–(S)–Phe–OH, Boc–(S)–Leu–OH, and Boc–(S)–Val–OH (note the formal change of configuration assignment upon homologation), respectively.[19,20] Peptide couplings were mediated by *N*,*N*′-dicyclohexylcarbodiimide and 1-hydroxy benzotriazole.[18] Crude peptide **1** was purified by medium-pressure liquid chromatography on a reverse-phase C_{18}(40–63 μ) column and crude peptide **2** was purified by high pressure liquid chromatography (HPLC) on a C_{18} (5–10 μ) column using methanol–water gradients.

Peptides were characterized by electrospray ionization–mass spectroscopy (ESI-MS)**:** Peptide **1,** M + H^+ = 1033.7 Da and M + Na^+ = 1055.6 Da (M calc = 1032 Da; Peptide **2 ,** M + Na^+ =1083.6 Da (M calc = 1060 Da) and complete analysis of the 500-MHz ^{1}H-NMR spectrum. Single crystals suitable for X-ray diffraction for peptide **1** were obtained by slow evaporation from ethanol–toluene–xylene solvent mixtures. The synthesis and characterization of peptide **3** has been previously described.[15]

X-Ray Diffraction

Crystals in the form of thin plates were obtained by slow evaporation from ethanol containing some toluene and xylene. A crystal, 1.00 × 0.56 × 0.06 mm in size, was used to collect X-ray diffraction data on a Bruker Smart CCD 6K diffractometer. A high intensity rotating anode (Cu radiation) X-ray source was used to collect data to a preset limit of $\theta = 67^\circ$ (0.84 Å resolution) at −75°C. Even at the limit of the setting of the apparatus, there were reflections with usable intensities. However, the structure solution was not automatic, possibly because the *hkl* reflections with $h = 2n$ were much stronger than those with $h \neq 2n$. A vector search procedure based on a hairpin model taken from the decapeptide Boc–Leu–Val–βPhe–Val–D-Pro–Gly–Leu–βPhe–Val–Val–OMe molecule was not successful, in retrospect, possibly because the β-turns are of different types in the two crystals. However, 15,000 trials with the SHELX program[21] led to a successfully placed fragment that was used with the tangent formula expansion[22] to obtain the entire structure consisting of two independent peptide molecules and two ethanol solvent molecules in an asymmetric unit. Hydrogen atoms were placed in idealized positions and allowed to ride on the C or N atom to which they are bonded. Anisotropic least-squares refinement produced an *R* factor of 7.5% for 14439 data with $|F_{obs}| > 4\sigma(F_0)$ and 8.7% for all 17,056 data. For the crystal with a formula content of $2(C_{55}H_{84}N_8O_{11}) \cdot 2(C_2H_5OH)$, the crystallographic parameters are: space group $P2_1$, a = 19.555(1) Å, b = 11.352(1) Å, c = 28.912(1) Å, β=101.909(2)°, V = 6259.8(4) Å^3, $Z = 4$, $d_{calc} = 1.145$ gm/cm^3.

Details of data collection, coordinates, bond lengths and angles, anisotropic thermal parameters, and hydrogen coordinates are deposited in the Cambridge Crystallographic Data Centre, Cambridge CB2 1EZ, UK, ref. CCDC #225008.

RESULTS AND DISCUSSION

Conformational Analysis of Peptide 1 in the Solid State

The conformations of the two crystallographically independent molecules A and B of peptide **1**, molecule A shown in stereo in Figure 2, are very similar, but not identical. There are four areas of significant differences, that is, more than 30° in the torsional angles that are listed in Table I. In the backbone, three differences occur at ψ_3, 37° for the $N_3C_{3A}C'_3N_4$ torsion just preceding the D-Pro residue; at ψ_5, 33° for the $N_5C_{5A}C'_5N_6$ torsion; and at ϕ_6, 33° for the $C'_5N_6C_{6A}C'_6$

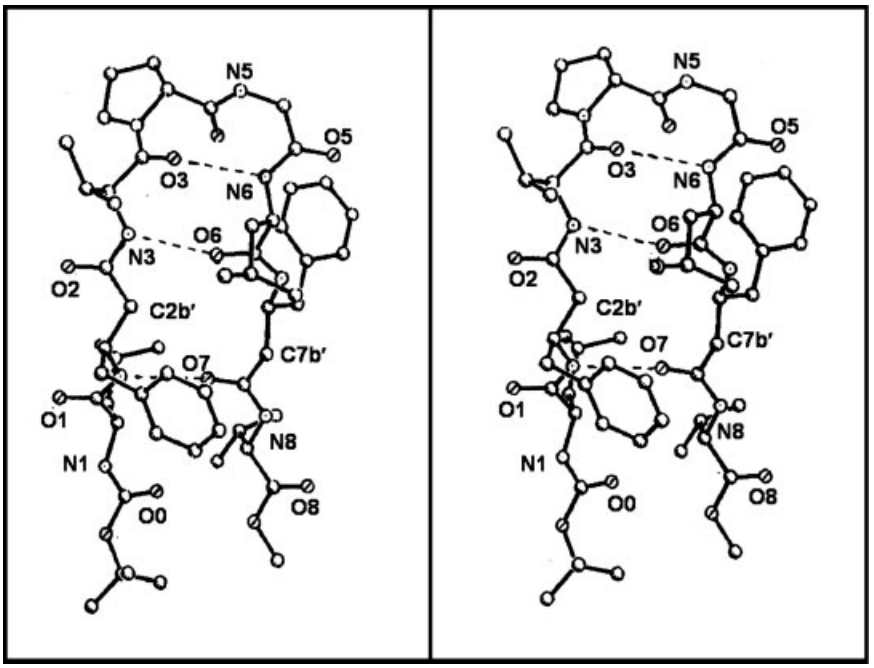

FIGURE 2 Stereodiagram of conformer A of Boc–Leu–βPhe–Val–D-Pro–Gly–Leu–βPhe–Val–OMe (peptide **1**).

torsion. In the side chains there is one difference at Val 3 where the rotation about C_{3A}–C_{3B} is *gauche*$^+$ in one conformer and *gauche*$^-$ in the other. All these differences occur in the vicinity of the hairpin turn. Despite the differences in several of the torsional angles, the hydrogen bonds in both conformers A and B are essentially the same, both cross-strand, Figure 2, and intermolecular, Table II.

Table I Torsion Angles For Peptide 1[a]

	Torsion Angles (°)					
Residue Name	ϕ	θ	ψ	χ^1	χ^2	χ^3
Leu 1	−94.4		125.6	176	63.7, −174.1	
	(−113.9)		(125.5)	(173.4)	(62.7, −175.5)	
βPhe 2	−141.1	150.2	158.8	56.3	−76.7, 99	
	(−145.4)	(160.5)	(151.1)	(54.6)	(−78.2, 100.7)	
Val 3	−153.7		122.6	50, 179.1		
	(−139.3)		(86.3)	(−45.4, −169.7)		
D-Pro 4[b]	55.7		−130.5	21.6	−28.9	24.2
	(64.5)		(−122.2)	(11.2)	(−29.1)	(35.2)
Gly 5	−83.3		20.4			
	(−73.1)		(−11.5)			
Leu 6	−117.6		113.1	170.5	58.6, −176.2	
	(−85.8)		(109.2)	(174.2)	(−175.9, 57.3)	
βPhe 7	−101	166.7	118.5	−50.1	150.8, −26.5	
	(−91.9)	(166.3)	(115.5)	(−58.9)	(−15.3, 163.6)	
Val 8	−156.8		143.8[c]	57.8, −174.1		
	(−154.8)		(122.2[c])	(179, 54.4)		

[a] The torsion angle values given without parentheses are for molecule A and the torsion angle values given inside parentheses are for molecule B.

[b] χ4: −9.7 (−29.3); χ^5 (Cδ—N—Cα—Cβ): −7.7 (11.4).

[c] Torsion around N8—C8—C8′—O9.

Table II Hydrogen Bonds in Peptide 1

H-Bond Type	Donor[a]	Acceptor[a]	d(D···A) (Å)	d(H···A) (Å)	D···O=C Angle (°)
Intramol.	N2 (Mol A)	O7 (Mol A)	2.92	2.02	175.61
Intramol.	N3 (Mol A)	O6 (Mol A)	2.91	2.04	161.45
Intramol.	N6 (Mol A)	O3 (Mol A)	2.93	2.06	160.40
Intramol.	N12 (Mol B)	O17 (Mol B)	2.95	2.06	171.88
Intramol.	N13 (Mol B)	O16 (Mol B)	2.82	1.93	172.90
Intramol.	N16 (Mol B)	O13 (Mol B)	2.99	2.15	155.83
Intramol.	N1 (Mol A)	O18 (Mol B)	2.96	2.13	152.84
Intramol.	N7 (Mol A)	O12[b] (Mol B)	2.95	2.05	175.24
Intramol.	N8 (Mol A)	O11[b] (Mol B)	2.94	2.06	161.37
Intramol.	N11 (Mol B)	O8[c] (Mol A)	3.02	2.13	167.96
Intramol.	N17 (Mol B)	O2 (Mol A)	2.95	2.06	169.36
Intramol.	N18 (Mol B)	O1 (Mol A)	2.94	2.05	171.60
EtOH–pept.	O1ET	O4	2.69		
EtOH–pept.	O2ET	O14	2.76	1.91	179.46
EtOH–pept.	N5	O1ET[d]	2.83	1.93	173.81
EtOH–pept.	N15	O2ET[e]	2.85	1.96	170.66

[a] For assignments, see Figure 2 and Figure 4.
[b] At symmetry equivalent $x-1, +y, +z$.
[c] At symmetry equivalent $x+1, +y, +z$.
[d] At symmetry equivalent $-x+1, +y+1/2, -z+1$.
[e] At symmetry equivalent $-x+2, +y+1/2, -z+1$.

Figure 3 compares the structures determined previously for the decapeptide, Boc-Leu-Val-βPhe-Val-D-Pro-Gly-Leu-βPhe-Val-Val-OMe, which differs from peptide **1** in having an additional Val residue at both the N and C-termini. The decapeptide hairpin has four intramolecular hydrogen bonds, whereas peptide **1** has three intramolecular hydrogen bonds. The nature of the nucleating turn differs in the two cases. In peptide **1**, a type II′ turn has formed, a feature found commonly in hairpins, whereas in the decapeptide, a type I′ turn is seen. The superposition of structures shown in Figure 3 clearly illustrates the differences in orientation of the turns in two cases. In each case, the NH and C=O moieties at the top of the hairpin participate in hydrogen bonding with mediating solvent molecules. In the direction lateral to the β-hairpins, hydrogen bonds between the strands of separate molecules link them into infinite β-sheets in both peptide **1** and the decapeptide crystals. The individual hairpins in peptide **1** have their headgroups pointed in the same direction (Figure 4).

A view of the crystal structure of **1** edge-on to the β-sheets is shown in Figure 5. There is a continuous vertical connection between alternating right and left hairpin molecules by an EtOH molecule that forms an OH · · · O=C hydrogen bond with the peptide ''head'' of the molecule below [O1EA · · · O4] and an O · · · HN with the peptide ''head'' of the molecule above [O1EA · · · N5]. At the ''tail-to-tail'' region, there is a slight interdigitation of the nonpolar tails (not shown).

NMR Analysis of Peptide 1

Peptide **1** yields a sharp 500-MHz ^{1}H-NMR spectrum in methanol-d_3 (CD_3OH). In chloroform and benzene, a broad spectrum, characteristic of aggregated species, are observed. Addition of a small amount of (5.66% v/v) methanol to $CDCl_3$ results in sharpening of NH resonances. All subsequent studies were done in neat CD_3OH at a peptide concentration of ($\sim$6.8 m*M*), at which aggregation effects are insignificant. Sequence-specific assignments of the amide resonances were readily achieved using total correlation spectroscopy (TOCSY) and rotating frame nuclear Overhauser spectroscopy (ROESY) experiments. The relevant NMR parameters are summarized in Table III. The large $^3J_{NH—C^{\alpha}H}$ values (for α residues) are consistent with extended strand conformations for residues 1–3 and 6–8. The observation of the Val 3 (NH) $\leftrightarrow$ Leu 6 (NH) NOE (d_{NN} NOE) supports the antiparallel registry of the two strands (Figure 6). The strong Gly 5 (NH) $\leftrightarrow$ Leu 6 (NH) NOE (d_{NN} NOE) is characteristic of the Gly residue occupying the $i+2$ position of a β-turn. The strong NOE between D-Pro 4 ($C^{\alpha}H$) and Gly 5 (NH) ($d_{\alpha N}$ NOE) is supportive of a ψ value $\sim +120^{\circ}$ at D-Pro 4, providing support for a D-Pro–Gly type II′ β-turn. A weak NOE

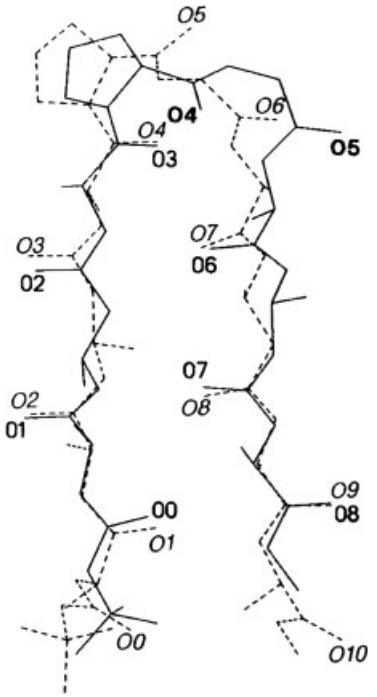

FIGURE 3 Superposition of peptide **1** (solid line) and Boc–Leu–Val–βPhe–Val–D-Pro–Gly–Leu–βPhe–Val–Val–OMe (dashed line) by least-squares fit of corresponding C^{α} atoms in the strands. Note the differences between type I′ β-turn for Boc–Leu–Val–βPhe–Val–D-Pro–Gly–Leu–βPhe–Val–Val–OMe and type II′ β-turn for peptide **1.**

between Leu 1 (NH) and Val 8 ($C^{\alpha}H$) (Figure 6) is notable. This NOE may arise when Leu1 (NH) points inward into the hairpin. The strong Leu 1 (NH) $\leftrightarrow$ βPhe 2 (NH) NOE suggests that local helical conformations may also be populated. It should be noted that the orientations of the Leu 1 and Val 8 residues are essentially unconstrained by hairpin formation. Interestingly, in the crystal structure of peptide **1**, both Leu 1 and Val 8 adopt extended conformations:

Leu 1 $\phi = -94.4^{\circ}$, $\psi = 125.6^{\circ}$(molecule A),
$\phi = -113.9^{\circ}$, $\psi = 125.5^{\circ}$ (molecule B).
Val 8 $\phi = -156.8^{\circ}$, $\psi = 143.8^{\circ}$ (molecule A),
$\phi = -154.8^{\circ}$, $\psi = 122.2^{\circ}$ (molecule B).

(Note Val 8 ψ is determined using the coordinate of the oxygen atom of the terminal OMe group as the fourth atom.)

This is undoubtedly a consequence of the formation of intermolecular β-sheet hydrogen bonds involving the backbone NH and CO groups of Leu 1 and Val 8 residues. Figure 7 shows a schematic view of the hairpin in peptide **1,** illustrating the major NOEs diagnostic of a β-hairpin structure.

NMR Analysis of Peptide 2

Peptide **2** yielded broad backbone resonances in $CDCl_3$ solution, indicative of extensive aggregation. Sharp, well-resolved 500-MHz ^{1}H-NMR spectra were obtained in deuterated methanol (CD_3OH) solution. Resonance assignments were readily achieved using a combination of TOCSY and ROESY experiments. The relevant NMR parameters are summarized in Table IV. Figure 8 shows a partial ROESY spectrum illustrating key NOEs. The observation of the Phe 2 (NH) $\leftrightarrow$ Phe 7 (NH) (d_{NN} NOE) is supportive of a

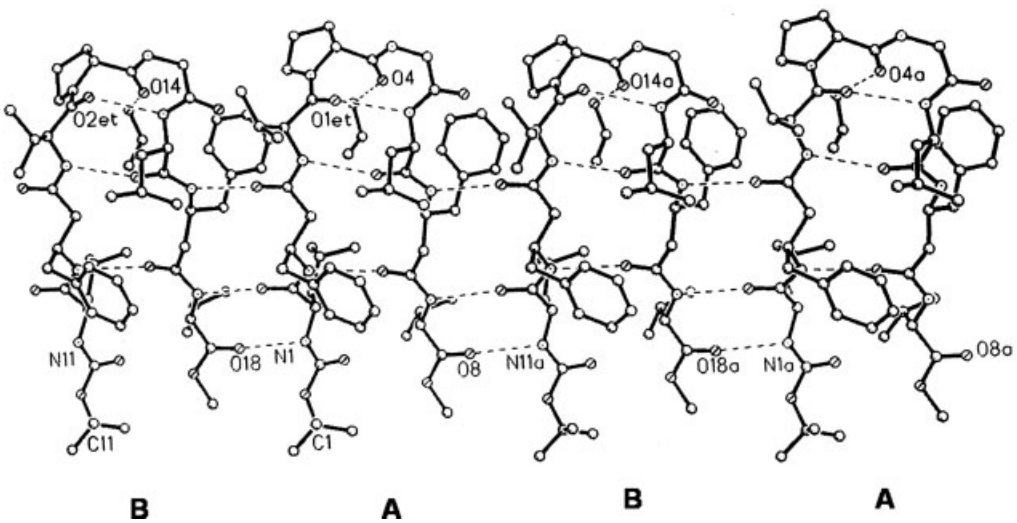

FIGURE 4 Assembly of peptide **1** conformers A and B into an extended β-sheet by intermolecular NH · · · OC hydrogen bonds. All the hairpin molecules have their ''head'' groups directed to the top of the diagram.

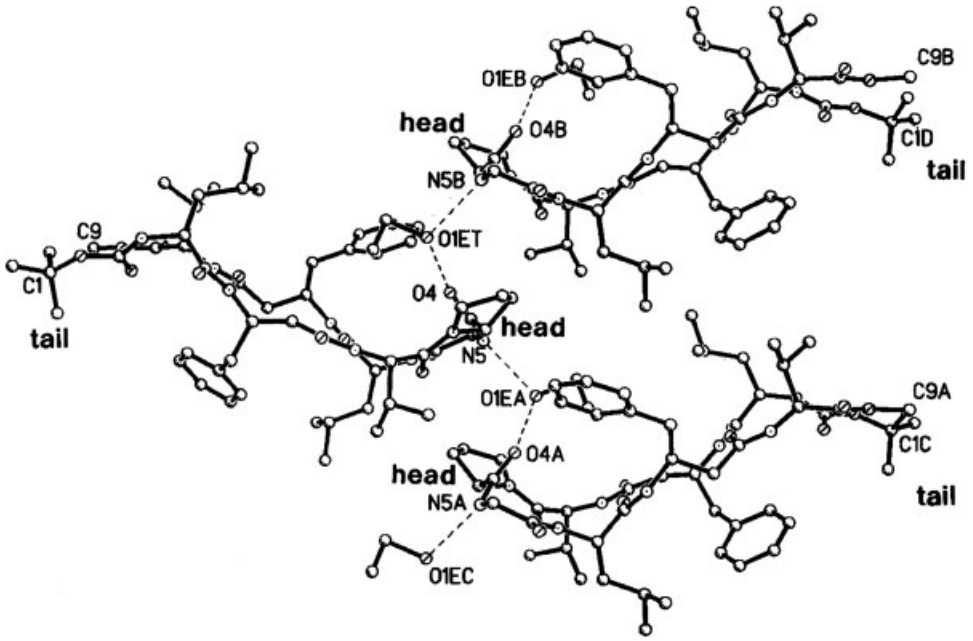

FIGURE 5 Packing viewed edge-on to the β-sheets in peptide **1**. The hydrogen bonds, mediated by EtOH molecules, in the polar ''head-to-head'' region are indicated.

β-hairpin structure. The NOE βVal 3 ($C^{\beta}H$) $\leftrightarrow$ βLeu 6 (NH) ($d_{\beta N}$ NOE) and βLeu 1 (NH) $\leftrightarrow$ βVal 8 ($C^{\beta}H$) ($d_{N\beta}$ NOE) also supports the antiparallel hairpin structure. The Gly 5 (NH) and βLeu 6 (NH) (d_{NN} NOE) is indicative of the anticipated chain reversal at the D-Pro–Gly segment. The NOEs supportive of a β-hairpin in peptide **2** are schematically illustrated in Figure 7. Interestingly, a strong D-Pro 4 ($C^{\alpha}H$) $\leftrightarrow$ Gly 5 (NH) ($d_{\alpha N}$ NOE) and a weak D-Pro 4 ($C^{\delta}H$) $\leftrightarrow$ Gly 5 (NH) ($d_{\delta N}$ NOE) are both observed. The simultaneous observation of these NOEs suggests that both type I′ and type II′ β-turn conformations are populated at the D-Pro–Gly turn segment. While the majority of D-Pro–Gly turn segments characterized crystallographically in peptide β-hairpins adopt type II′ conformations, type I′ turns have also been observed.[16,18] The weak d_{NN} NOEs βLeu 1 (NH) $\leftrightarrow$ Phe 2 (NH), Phe 2 (NH) $\leftrightarrow$ βVal 3 (NH), and Phe 7 (NH) $\leftrightarrow$ βVal 8 (NH) are not compatible with a completely rigid hairpin and suggest fraying of the structure at the N- and C-terminus ends. Such fraying is a relatively common feature in CD_3OH solution, since solvent competition for backbone hydrogen-bonding sites tends to destabilize the hairpins.

Table III ^{1}H-NMR Parameters for Peptide 1 in CD_3OH at 300 K

	δ (ppm)						
Residue Name	NH	$C^{\alpha}H$	$C^{\beta}H$	$C^{\gamma}H$	$C^{\delta}H$	Others	$^3J_{NH—C^{\alpha}H}$ (Hz)[a]
Leu 1	6.51	4.08	$C^{\beta}H_2/C^{\gamma}H$ (1.57/1.34)		0.88		8.7
βPhe 2	7.98	2.50	4.50	2.78, 2.87		aromatic: ~7.25	8.8[b]
Val 3	8.36	4.53	2.10	1.00			7.5
D-Pro 4	—	4.36	$C^{\beta}H_2/C^{\gamma}H_2$ (2.03, 2.16/2.26)		3.74, 3.89		—
Gly 5	8.41	3.80, 3.88					—
Leu 6	8.05	4.38	$C^{\beta}H_2/C^{\gamma}H$ (1.51, 1.74)		0.92		8.4
βPhe 7	7.95	2.50	4.44	2.75, 2.85		aromatic: ~7.25	8.6
Val 8	8.28	4.43	2.15	0.95			8.3

[a] For β-residues, the vicinal coupling constant ($^3J_{NH—C^{\alpha}H}$) is given.

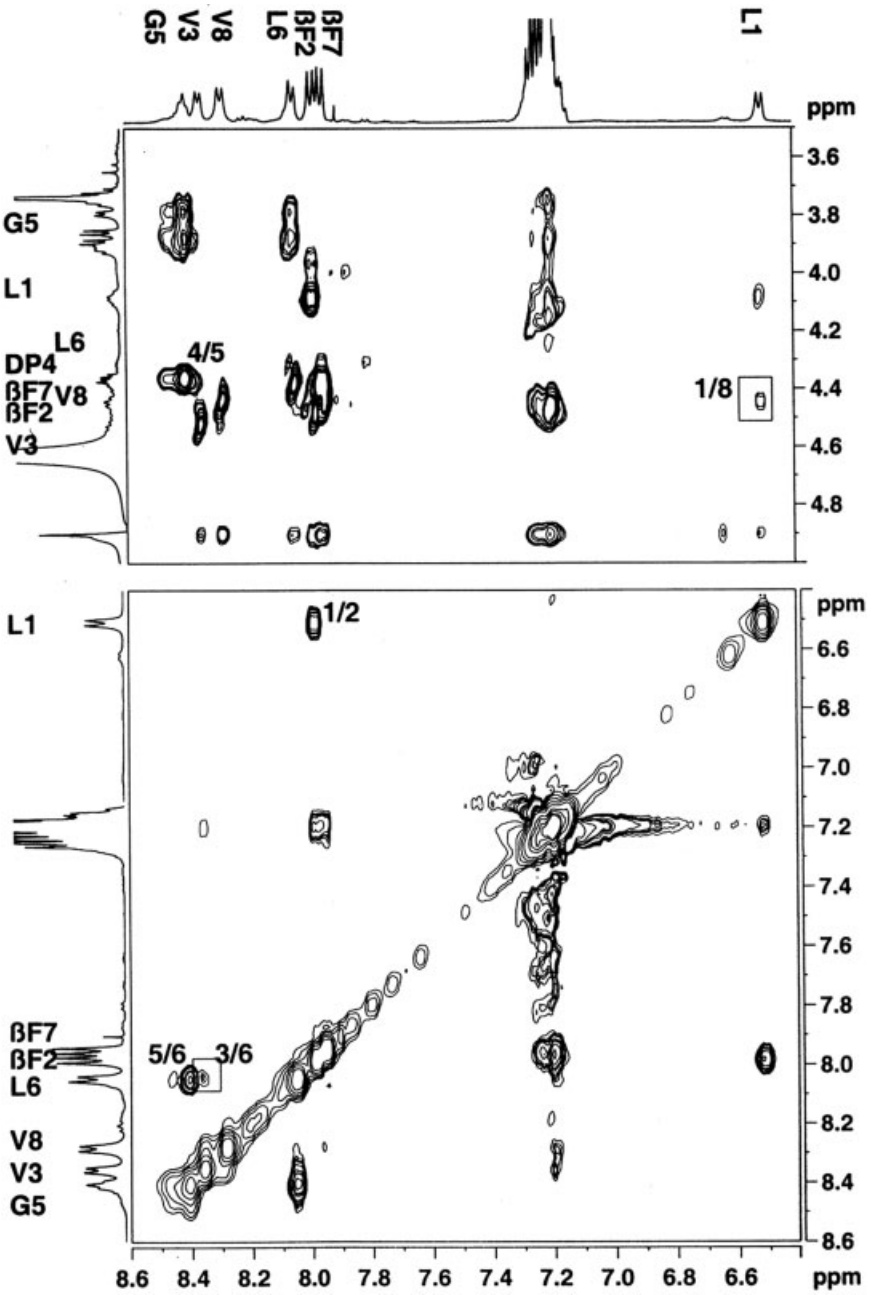

FIGURE 6 Partial 500-MHz ROESY spectrum of Boc–Leu–βPhe–Val–D-Pro–Gly–Leu–βPhe–Val–OMe (**1**) in CD_3OH at 300 K. (Top) $C^{\alpha}H \leftrightarrow NH$ NOEs (α-residues) and $C^{\beta}H \leftrightarrow NH$ NOEs (β-residues). (Bottom) NH $\leftrightarrow$ NH NOEs. Key NOEs are marked.

Circular Dichroism. Figure 9 illustrates the CD spectra for peptides **1**–**3** in methanol solution. Peptide **1** has a broad negative CD band with a minimum at 224 nm. The CD spectra of model peptide β-hairpins that do not contain aromatic residues have been shown to yield a broad negative band at 214–220 nm.[8,14,15,23,24] The origins of the red shift in the case of **1** is not clear. It is conceivable that this is a consequence of the fact that the strand residues are made up of both α- and β-amino acids, resulting in differences in the orientation of peptide chromophores as compared to all α-peptide cases. Notably, the CD spectrum of peptide **2** is anomalous, yielding a negative band at 234 nm and a positive band at 221 nm. This observation may be rationalized by invoking an exciton interaction between the phenyl chromophores of Phe 2 and Phe 7. A comparison of the CD spectrum of peptide **2** with that of parent

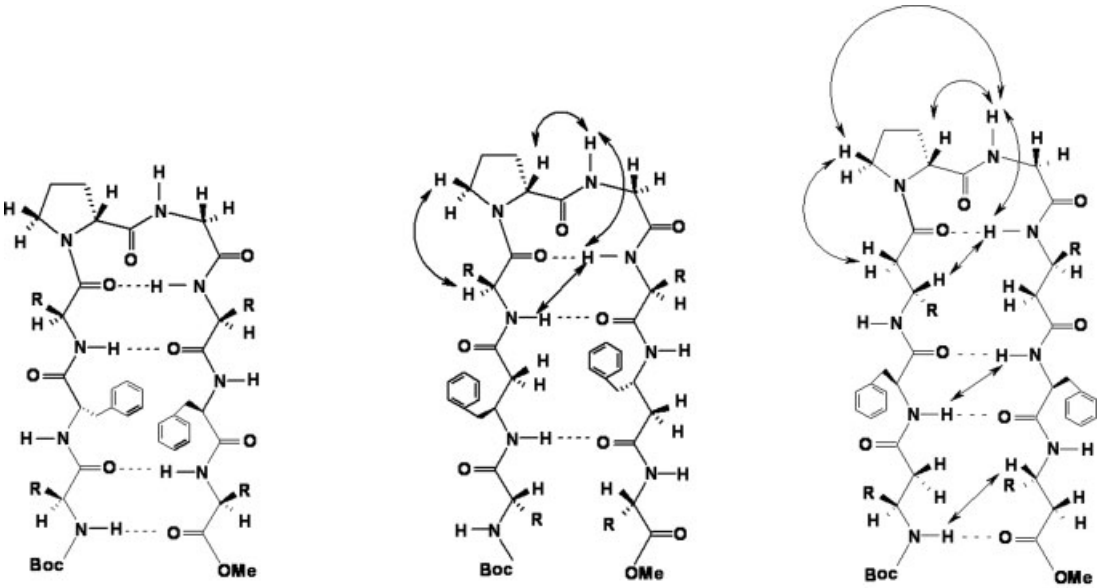

3 **1** **2**

FIGURE 7 Schematic representation of hairpin structures for peptides **3, 1,** and **2** illustrating key NOEs, which are consistent with the hairpin conformation. For other NOEs, see the text.

peptide **3** is also instructive. In peptide **3**, negative bands are observed at 235 and 210 nm (Figure 9).[15] A positive band at 224 nm overlapped with a lower wavelength negative CD band may be the reason for nonobservation of an exciton split doublet, which is seen for peptide **2** and also for octapeptide Boc–Leu–Phe–Val–Aib-D-Ala–Leu–Phe–Val–OMe.[14] Figure 9 also illustrates the orientation of the facing aromatic residues observed in crystals of peptide **1** and the β- hairpin segment corresponding to the segment of peptide **3** in a 17-residue helix–hairpin peptide. In peptide **1**, the centroid-to-centroid distance between the aromatic rings are 8.92 Å (for molecule A) and 8.94 Å (for molecule B). The corresponding distance between facing Phe residues in the *nonhydrogen-bonded* position determined for the Boc–Leu–Phe–Val–D-Pro–Gly–Leu–Phe–Val–OMe hairpin segment in a 17-residue peptide is 5.03 Å. In the crystal structure of Boc–Leu–Phe–Val–Aib-D-Ala–Leu–Phe–Val–OMe, the Phe–Phe centroid-to-centroid distance is 5.52 Å.[14] Crystals of peptide **2** suitable for X-ray diffraction were not obtained, despite several attempts. In order to estimate the interaromatic distance, Phe rings were modeled into the *hydrogen-bonding position* of a β-hairpin. Analysis of protein structures reveals that for most aromatic

Table IV ^{1}**H-NMR Parameters for Peptide 2 in CD_3OH at 300 K**

Residue	NH	$C^{\alpha}H$	$C^{\beta}H$	$C^{\gamma}H$	$C^{\delta}H$	$C^{\epsilon}H$	Others	$^3J_{NH-C^{\alpha}H}$ (Hz)[a]
βLeu 1	6.24	2.36, 2.45	3.94	$C^{\gamma}H_2/C^{\delta}H$ (1.09, 1.30, 1.61)		0.87		9.3
Phe 2	8.33	4.68	2.98, 3.12				Aromatic: ~7.25	8.1
βVal 3	7.84	2.34, 2.60	4.32	1.82	0.90			9.2
D-Pro 4	—	4.28	$C^{\beta}H_2/C^{\gamma}H_2$ (1.98/2.06/2.25)		3.63			—
Gly 5	8.51	3.80						—
βLeu 6	7.67	2.38, 2.66	4.39	$C^{\gamma}H_2/C^{\delta}H_2$ (1.10, 1.53, 1.63)		0.86		9.4
Phe 7	8.61	4.72	3.03,3.10				Aromatic: ~7.25	7.8
βVal 8	7.94	2.32,2.45	4.07	1.79	0.88			9.3

[a] For β-residues, the vicinal coupling constant ($^3J_{NH—C^{\alpha}H}$) is given.

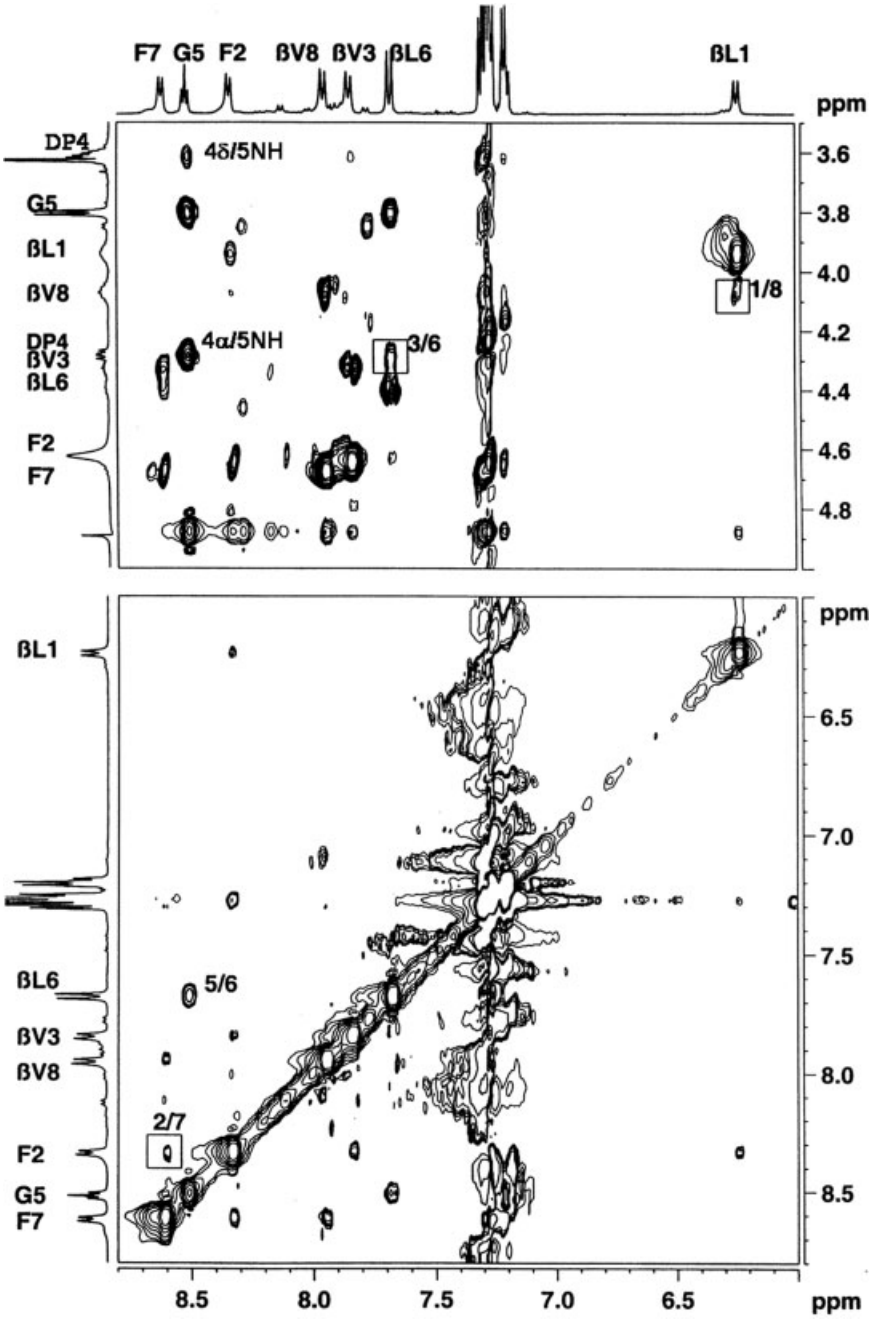

FIGURE 8 Partial 500-MHz ROESY spectrum of Boc–βLeu–Phe–βVal–D-Pro–Gly–βLeu–Phe–βVal–OMe (**2**) in CD_3OH at 300 K. (Top) $C^{\alpha}H \leftrightarrow$ NH NOEs (α-residues) and $C^{\beta}H \leftrightarrow$ NH NOEs (β-residues). (Bottom) NH $\leftrightarrow$ NH NOEs. Key NOEs are marked.

pairs at *hydrogen-bonding* sites in β-sheets, the favored combination of side-chain conformations are $g^{-}t$ and $g^{+}g^{-}$.[25,26] For $g^{+}g^{-}$ combination of side-chain torsion angles, aromatic rings are proximal [centroid-to-centroid distance: 4.78 Å] (Figure 9). However, in these orientations, the closest contact involves the C^{β} atom of one residue and the aromatic ring of the other.

Differences in the orientations of the two facing aromatic rings in peptides **1**–**3** are also evident from a comparison of the NMR chemical shifts of the aromatic proton resonances. From the data presented in Figure 10, it is clear that the aromatic protons in peptides **1** and **3** are shifted distinctly upfield, as compared to the corresponding resonances in peptide **2**. Indeed, in peptide **3**, there is an upfield shift of

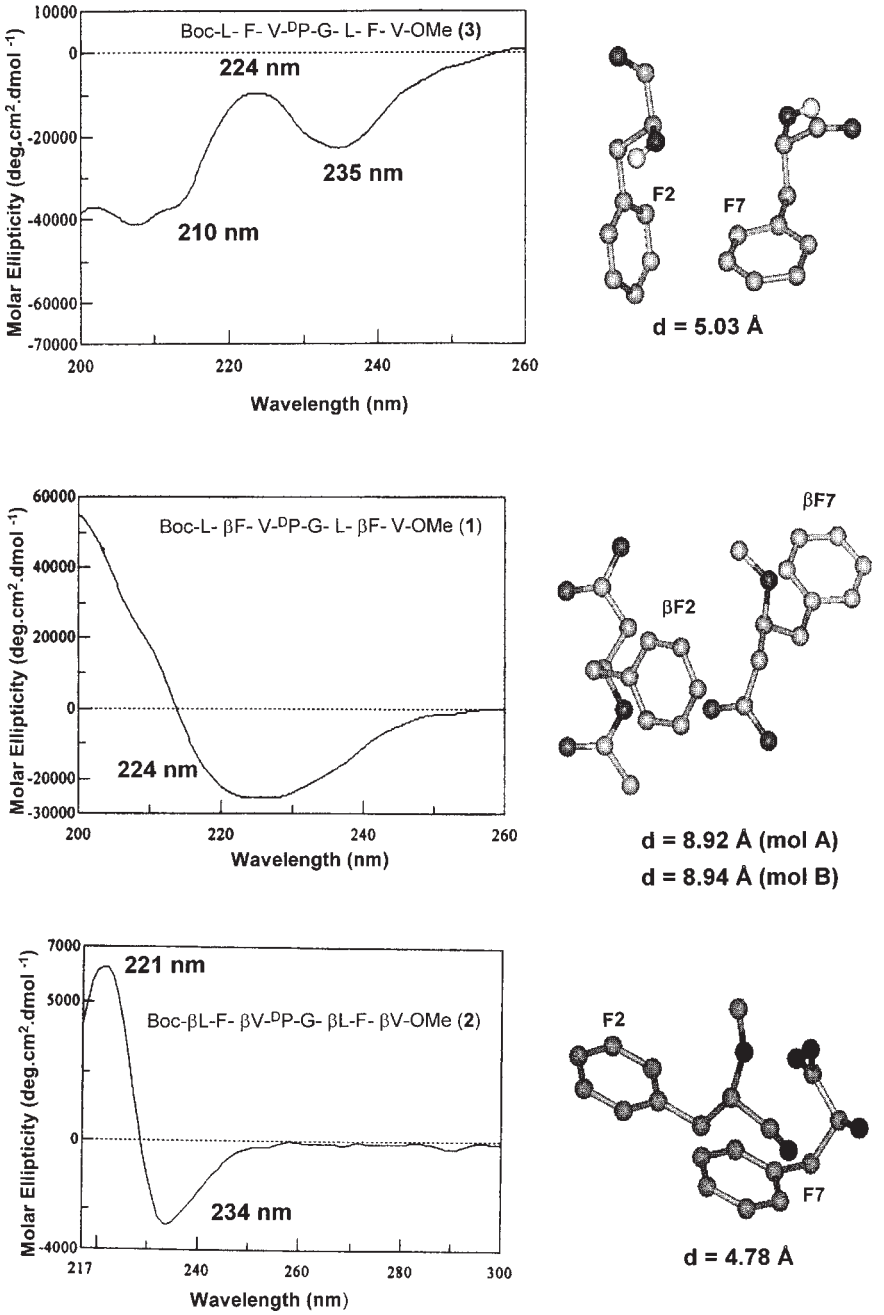

FIGURE 9 Far-UV CD spectra of peptides **3, 1,** and **2** in methanol at 300 K. The ''d'' refers to the centroid-to-centroid distance.

~0.4 ppm of the Phe 7 [H2 , H6] resonances. The ring current shifts observed for peptide **2** are much less pronounced. Interestingly, a small downfield shift is observed for the Phe ring proton resonances of peptide **2** as compared to peptide **1**. This feature is consistent with the interring orientation illustrated in Figure 9, which would place the aromatic protons of Phe 2 in the deshielding region of the proximal Phe 7 group. It is pertinent to note that the crystallographically determined Phe orientations in peptide **3** (Figure 9) places the $C^{\beta}H$ of Phe 2 in the *shielding* region of the aromatic ring current of Phe 7. Interestingly, for peptide **3**, the observed $C^{\beta}H_2$ proton chemical shifts reveal pronounced nonequivalence of the two Phe2 $C^{\beta}H_2$ protons (2.79, 3.12 ppm) as compared to Phe 7 $C^{\beta}H_2$ protons (2.85 ppm).

Aromatic interactions may have been frequently invoked as contributors to the stability of folded

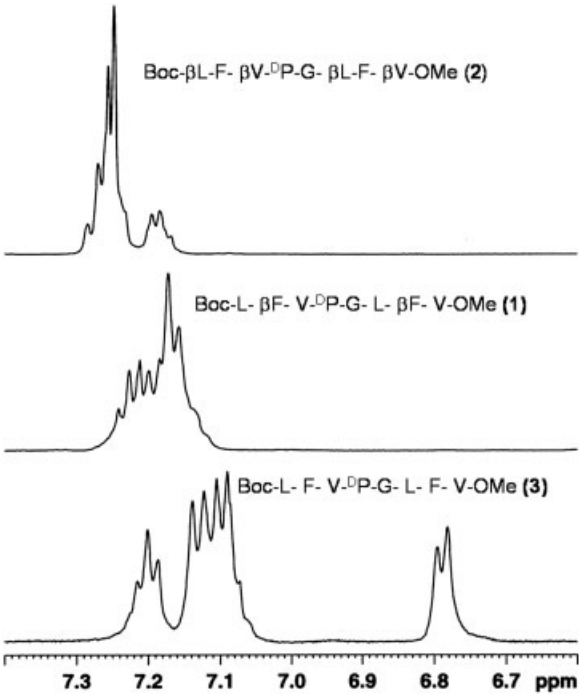

FIGURE 10 Partial 500-MHz ^{1}H-NMR spectra of peptides **3**, **1,** and **2** in CD_3OH at 300 K. Aromatic proton resonances are shown.

structures in proteins and peptides.[27–32] Analysis of interring orientation has revealed that there may be strong preference for either stacked (interplanar angle $= 0^\circ$) or perpendicular (interplanar angle $= 90^\circ$) ring orientation. A survey of Phe ring orientations in several peptide crystal structures is consistent with a broad energy minimum for an interacting aromatic pair and the absence of pronounced angular dependence. These observations are also consistent with the result of theoretical calculations for interacting benzene rings.[33] Aromatic interactions are generally considered to be stabilizing for interring distances ~4.5–7 Å.[34,35] It is likely that the close approach of aromatic rings may result in anomalous CD. In addition to proximity, restriction of side-chain mobility and adoption of a fixed rotamer about the C^α—C^β may also be contributors to the observed CD.

CONCLUSIONS

Defined peptide hairpins provide an opportunity to explore side-chain interactions in β-sheet structures. The result presented here establish that aromatic interactions may be important contributors to the observed circular dichroism, when residues involved occupy facing positions across a pair of antiparallel strands. Anomalous CD spectra are observed when the interacting pair occupies either *hydrogen-bonding* or *nonhydrogen-bonding* positions in an antiparallel sheet. Our results emphasize the utility of D-Pro–Gly segments in nucleating hairpins in hybrid peptide containing α- and β-amino acids. The utility of mixed α/β-sequences in altering side-chain dispositions in designed peptides is also exemplified in the structures described here.

This work was supported in Bangalore by a program support grant in the area of Molecular Diversity and Design by the Department of Biotechnology, Government of India. RSR is a recipient of a senior research fellowship of the Council of Scientific and Industrial Research, Government of India. The work at the Naval Research Laboratory was supported by National Institutes of Health Grant GM30902 and the office of Naval Research. We thank Ms Pratima Iyenger, Ms. R. Sathyapriya, and Mr. J. Rajan Prabhu for their help in generating Figure 9. We thank Mr. Siddartha Roy for his help in making Table II.

REFERENCES

1. Awasthi, S. K.; Raghothama, S.; Balaram, P. Biochem Biophys Res Commun 1995, 216, 375–381.
2. Haque, T. S.; Little, J. C.; Gellman, S. H. J Am Chem Soc 1994, 116, 4105–4106.
3. Raghothama, S.; Awasthi, S. K.; Balaram, P. J Chem Soc Perkin Trans 2, 1998, 137–143.
4. Gellman, S. H. Curr Opin Chem Biol 1998, 2, 717–725.
5. Venkatraman, J.; Shankaramma, S. C.; Balaram, P. Chem Rev 2001, 101, 3131–3152.
6. Venkatraman, J.; Naganagowda, G. A.; Balaram, P. J Am Chem Soc 2002, 124, 4987–4994.
7. Das, C.; Raghothama, S.; Balaram, P. J Chem Soc 1998, 120, 5812–5813.
8. Das, C.; Shankaramma, S. C.; Balaram, P. Chem Eur J 2001, 7, 840–847.
9. Karle, I. L.; Awasthi, S. K.; Balaram, P. Proc Natl Acad Sci USA 1996, 93, 8189–8193.
10. Karle, I. L.; Das, C.; Balaram, P. Proc Natl Acad Sci USA 2000, 97, 3034–3037.
11. Das, C.; Naganagowda, G. A.; Karle, I. L.; Balaram, P. Biopolymers 2001, 58, 335–346.
12. Aravinda, S.; Harini, V. V.; Shamala, N.; Das, C.; Balaram, P. Biochemistry 2004, 43, 1832–1846.
13. Aravinda, S.; Shamala, N.; Roy, R. S.; Balaram, P. Proc Ind Acad Sci (Chem Sci) 2003, 115, 373–400.
14. Aravinda, S.; Shamala, N.; Rajkishore, R.; Gopi, H. N.; Balaram, P. Angew Chem Intl Ed 2002, 41, 3863–3865.
15. Zhao, C.; Polavarapu, P. L.; Das, C.; Balaram, P. J Am Chem Soc 2000, 122, 8228–8231.
16. Karle, I. L.; Gopi, H. N.; Balaram, P. Proc Natl Acad Sci USA 2001, 98, 3716–3719.

17. Karle, I. L.; Gopi, H. N.; Balaram, P. Proc Natl Acad Sci USA 2002, 99, 5160–5164.
18. Gopi, H. N.; Roy, R. S.; Raghothama, S.; Karle, I. L.; Balaram, P. Helv Chim Acta 2002, 85, 3313–3330.
19. Seebach, D.; Overhand, M.; Kuhnle, F. N. M.; Martini, B.; Oberer, L.; Hommel, U.; Widmer, H. Helv Chim Acta 1996, 79, 91–941.
20. Pluncinska, K.; Liberek, B. Tetrahedron 1987, 43, 3509–3517.
21. Sheldrick, G. M. Acta Cryst 1990, A46, 467–473.
22. Karle, J. Acta Cryst 1968, B24, 182–186.
23. Alvardo, M. R.; Blanco, F. J.; Serrano, L. Nat Struct Biol 1996, 3, 604–612.
24. Maynard, A. J.; Sharman, G. J.; Searle, M. S. J Am Chem Soc 1998, 120, 1996–2007.
25. Hutchison, E. G.; Sessions, R. B.; Thronton, J. M.; Woolfson, D. N. Protein Sci 1998, 7, 2287–2300.
26. Chakrabarti, P.; Pal, D. Prog Biophys Mol Biol 2001, 76, 1–102.
27. Burley, S. K.; Petsko, G. A. Adv Prot Chem 1988, 39, 125–189.
28. Waters, M. L. Curr Opin Chem Biol 2002, 6, 736–741.
29. Thomas, A.; Meurisse, R.; Charloteaux, B.; Brasseur, R. Proteins Struct Funct Genet 2002, 48, 628–634.
30. Thomas, A.; Meurisse, R.; Brasseur, R. Proteins Struct Funct Genet 2002, 48, 635–644.
31. Singh, J.; Thornton, J. M. FEBS Lett 1985, 191, 1–6.
32. Hunter, C. A.; Singh, J.; Thronton, J. M. J Mol Biol 1991, 218, 837–846.
33. Sinnokrot, M. O.; Valeev, E.; Sherrill, C. D. J Am Chem Soc 2002, 124, 10887–10893.
34. Burley, S. K.; Petsko, G. A. Science, 1985, 229, 23–28.
35. Aravinda, S.; Shamala, N.; Das, C.; Sriranjini, A.; Karle, I. L.; Balaram, P. J Am Chem Soc 2003, 125, 5308–5315.